

# Thermally conductive self-healing nanoporous materials based on hydrogen-bonded organic frameworks

Muhammad Akif Rahman, C. Jaymes Dionne, and Ashutosh Giri\*

*Department of Mechanical Industrial and Systems Engineering, University of Rhode Island,  
Kingston, RI 02881, USA*

E-mail: ashgiri@uri.edu

## Abstract

Hydrogen-bonded organic frameworks (HOFs) are a class of nanoporous crystalline materials formed by the assembly of organic building blocks that are held together by a network of hydrogen-bonding interactions. Herein, we show that the dynamic and responsive nature of these hydrogen-bonding interactions endows HOFs with a host of unique physical properties that combine ultra-flexibility, high thermal conductivities, and the ability to ‘self-heal’. Our systematic atomistic simulations reveal that their unique mechanical properties arise from the ability of the hydrogen-bond arrays to absorb and dissipate energy during deformation. Moreover, we also show that these materials demonstrate relatively high thermal conductivities for porous crystals with low mass densities owing to their extended periodic framework structure that is comprised of light atoms. Our results reveal that HOFs mark a new regime of materials design combining multifunctional properties that make them ideal candidates for gas storage and separation, flexible electronics, and thermal switching applications.

**Keywords:** Hydrogen-bonded organic frameworks, ultraflexibility, high porosities, anisotropic thermal conductivity, and self-healable materials.

Multifunctional materials that combine extraordinary physical attributes such as being ultra-light weight, thermally conductive, superflexible and self-healable are crucial for the development of the next generation of technologies such as wearable electronics,<sup>1</sup> soft machines,<sup>2</sup> integrated circuits,<sup>3</sup> and flexible solar cells.<sup>4</sup> However, combining all of the aforementioned physical characteristics into one material system has proven to be one of the most fundamental scientific challenges. For example, thermally conductive materials are generally rigid and dense,<sup>5</sup> which limits their use in wearable electronics requiring highly flexible materials with low densities.<sup>6</sup> In this regard, porous crystals based on organic frameworks have pushed the envelope of materials design by combining some exceptional physical attributes.<sup>7–10</sup> These materials offer a unique platform for functional design mainly because of the vast diversity in the choice of their organic building blocks, which form extended frameworks with ordered nanopores that can be molded into different geometries and dimensions. Recently, we have shown that covalent organic frameworks (COFs) mark a new regime of materials design that combine ultralow mass densities and remarkably high thermal conductivities in porous crystals (Fig. 1).<sup>3,11</sup> Herein, we will show that another class of porous crystals based on hydrogen-bonded organic frameworks (HOFs) also possess high thermal conductivities with low mass densities (as shown in Fig. 1), all the while demonstrating a unique set of mechanical properties such as higher flexibilities and the ability to ‘self-heal’ after a catastrophic breakdown of the porous framework.

In general, porous crystalline solids have garnered tremendous attention over the past few decades, not just for the aforementioned applications but also for gas separation/storage, catalysis, chemical sensing, electrodes, and drug deliveries owing to their modular geometries and remarkably large surface areas.<sup>22–24</sup> HOFs are a class of such porous crystals that are largely inspired by the generality with which nature combines noncovalent supramolecular chemistry and covalent bonds in a variety of processes.<sup>10,25</sup> This combination endows HOFs with several advantages such as facile synthesis conditions, simple regeneration, and solution processability over other crystalline porous structures such as metal organic frameworks (MOFs) and COFs.<sup>10,26,27</sup> Moreover, these materials with supramolecular chemistries that are bridged by relatively weak

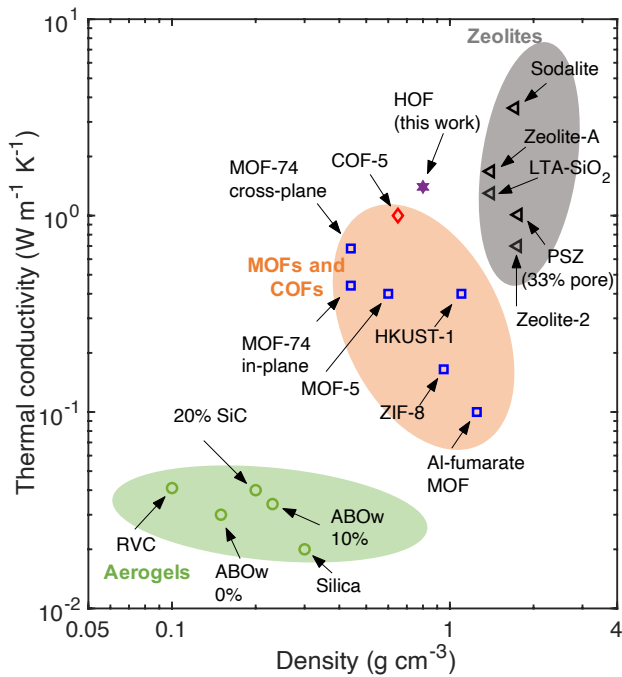


Figure 1: Comparison of thermal conductivities of various porous materials such as aerogels<sup>12</sup>, MOFs<sup>13–17</sup>, zeolites<sup>18–21</sup>, COF-5<sup>11</sup>, and ABTPA HOF (this work) as a function of mass density. Generally, zeolites have higher thermal conductivities since they have relatively higher mass densities as compared to other porous solids. Our HOF demonstrates comparable thermal conductivity to zeolites and higher thermal conductivity in comparison to aerogels and MOFs, while also possessing ultralow mass densities.

and reversible hydrogen bonds can easily adapt to their environment, thus potentially positioning them as shape-memory, self-healing and stimuli-responsive ‘smart materials’.<sup>28,29</sup> As such, their exceptional chemical and structural makeup should endow HOFs with multifunctional properties, yet the knowledge of their thermal and mechanical properties, (which are quintessential for their functionality in the aforementioned applications) have remained elusive thus far.

In terms of the understanding of thermal transport properties of nanoporous materials, the focus has mainly been limited to MOFs and zeolites.<sup>13,14,16,30–42</sup> Zeolites are generally shown to have higher thermal conductivities due to their relatively higher mass densities as shown in Fig. 1. For MOFs, most of the studies generally report very low thermal conductivities ( $\sim 0.3 \text{ W m}^{-1} \text{ K}^{-1}$ ), which has mostly been attributed to the short mean free paths of the vibrational energy carriers resulting from their porous structures. Similarly, aerogels also demonstrate some of the lowest thermal conductivities resulting from their highly porous structures. However, in contrast to these materials with a combination of ultralow thermal conductivities and mass densities, we recently measured a combination of high thermal conductivity ( $\sim 1 \text{ W m}^{-1} \text{ K}^{-1}$ ) and low mass density ( $0.55 \text{ g cm}^{-3}$ ) for COF-5, which we mainly attributed to the long range crystalline order and light atoms held together by strong covalent bonds.<sup>3</sup> In this work, our systematic atomistic simulations based on reactive molecular dynamics (MD) simulations show that HOFs are capable of possessing high thermal conductivities ( $>1 \text{ W m}^{-1} \text{ K}^{-1}$  at room temperature), which mainly depend on the orientation of their ultraflexible organic building blocks. We also show that HOFs possess the unique property of ‘self-healing’, where these materials are capable of recovering their physical attributes (such as their high thermal conductivity) even when the structure is severely fractured after the application of uniaxial strain. Furthermore, we reveal that HOFs are highly flexible and are capable of efficiently relieving stress under high levels of tensile strain. The stress relaxation under tensile loading in HOFs is attributed to the ability of the dynamic hydrogen bonds to absorb and efficiently localize the stress. Although the framework breaks down at high levels of strain ( $\sim 40\%$ ) under uniaxial tensile loading, the framework is shown to ‘self-heal’ through a counter strain that is applied in the lateral direction.

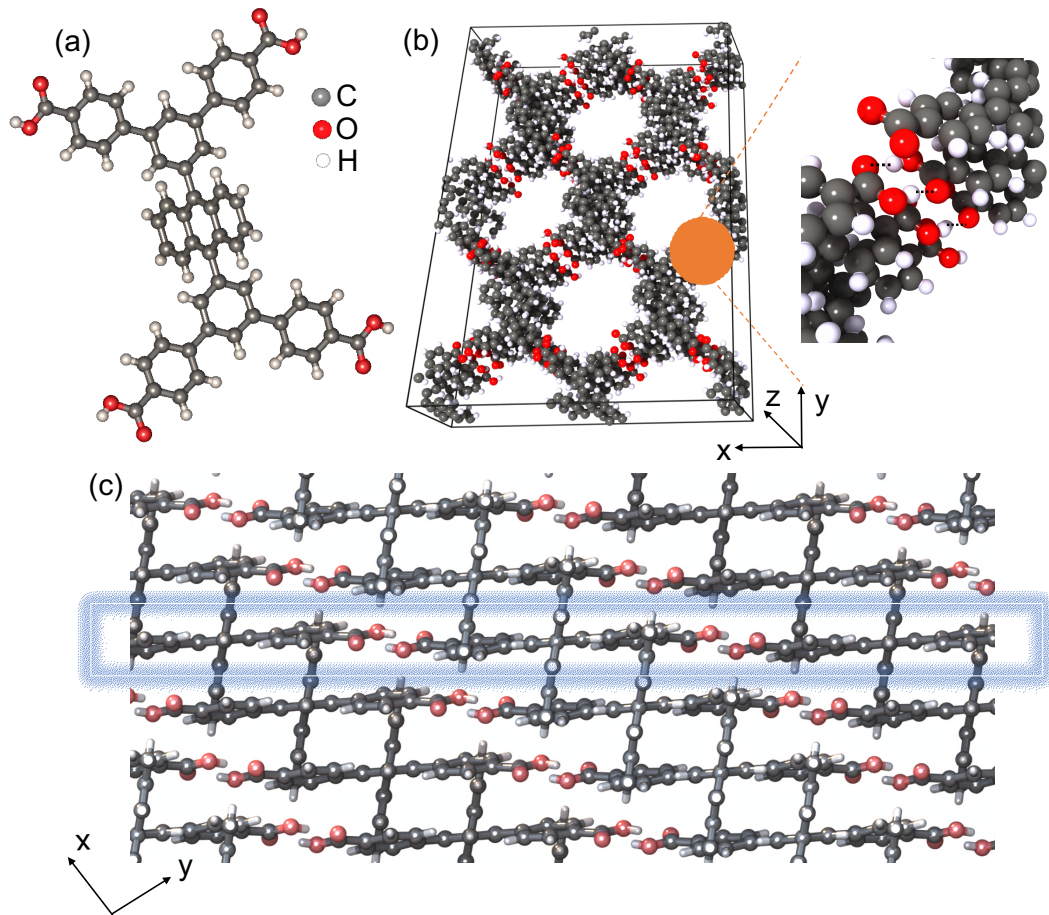


Figure 2: (a) Structure of the ABTPA building block of the HOF used in this work. (b) Schematic of our HOF computational domain with a magnified view of the hydrogen-bonding interactions ( $\text{O}-\text{H}\cdots\text{O}$ ). (c) The hydrogen bonds are aligned along a 2D lattice with the anthracene units packed in the out-of-plane direction.

We base our calculations on the recently synthesized ABTPA [5',5'''-(1,1'3',1"anthracene-9,10-diyl)bis([-ter 4,4"-phenyl]-dicarboxylic acid))] HOF, which has been recently synthesized by Cui *et al.*<sup>43</sup>; the chemical structure of the monomer building block is shown in Fig. 2a. We use a reactive potential, ReaxFF, to describe the interatomic interactions and conduct all of our simulations with the Large Atomic Molecular Massively Parallel Simulator (LAMMPS) package.<sup>44,45</sup> A distance-dependent bond order function is implemented in this potential. The reason we utilize the ReaxFF potential for all our simulations is in order to account for the significant role played by the dynamic and responsive behavior of the hydrogen-bonded interactions in our HOF structure that dictate their thermal and mechanical properties, as well as to accurately model the breaking and reforming of the bonds during our tensile deformation tests. The schematic of our computational domain is shown in the left panel of Fig. 2b. Each four-membered unit is held together by hydrogen-bonded interactions (O-H $\cdots$ O, as shown in the right panel of Fig. 2b). The ABTPA HOF has a 2D square lattice as highlighted in Fig. 2c with the anthracene units packed in the out-of-plane direction, which acts as an anchor for the 3D structure of the HOF.<sup>43</sup> This arrangement allows large flexibility in the dynamic movement of the organic building blocks and the free rotation of the anthracene units made possible by the hydrogen-bonded 2D square lattice. As such, this provides a potential avenue for an adaptive framework by introducing an overall responsive behavior of the HOF structure, which is what we seek to study by applying external strain as we detail below.

First, we calculate the temperature-dependent thermal conductivity of ABTPA HOF in the three principal directions via the Green-Kubo (GK) method as shown in Fig. 3. We also calculate the room temperature thermal conductivity in the *x*-direction for our HOF with a direct approach (i.e. the nonequilibrium MD method where we apply hot and cold baths to our simulation domains to create a temperature gradient; more details on the two approaches are given in the Supporting Information). The agreement between the two different approaches (within uncertainties) as shown in Fig. 3 provides confidence in our results.

The anisotropic structure of the HOF manifests in the direction-dependent thermal conductiv-

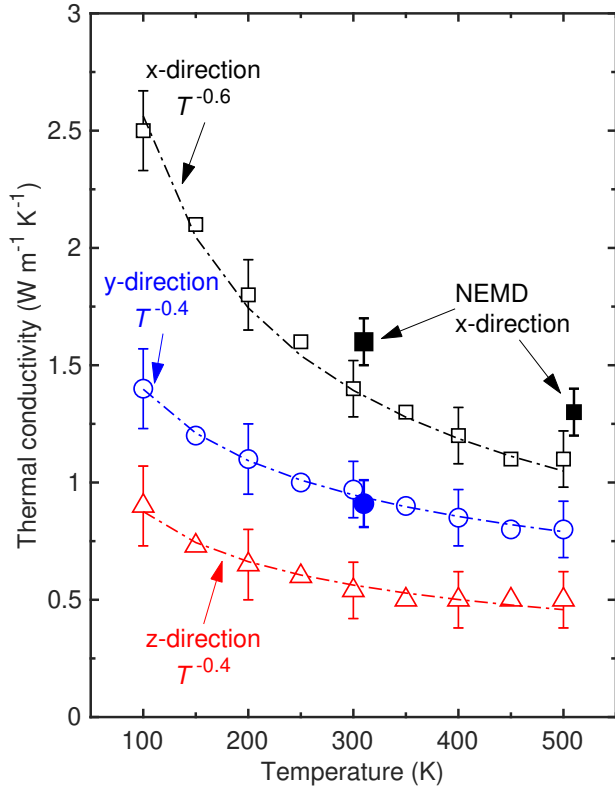


Figure 3: The ABTPA HOF possesses large anisotropy in the temperature dependent thermal conductivities along the three principal directions as calculated via the Green-Kubo approach. For comparison, we also include the calculations for the thermal conductivity along the  $x$ - and  $y$ -directions from our nonequilibrium molecular dynamics approach (solid symbols). The agreement between the two methods provides confidence in our calculations.

ties as shown in Fig. 3. The thermal conductivity is higher in the *x*-direction with a relatively larger temperature dependence, which is indicative of a more pronounced influence of anharmonic phonon-phonon scattering (or Umklapp scattering) effects in that direction. The deviation from the crystalline-like  $1/T$  temperature trend along all directions can be attributed to vibrational scattering at the pore walls of the HOFs. Since the characteristic length of the pore in the *x*-direction is shorter than the *y*-direction (see Fig. S1a), we can expect a more pronounced effect of pore-wall scattering and a reduced thermal conductivity along the *y*-direction. The larger temperature dependence for the *x*-direction in comparison to the *y*-direction is indicative of higher phonon-phonon scattering mechanisms dictating thermal conductivity along the *x*-direction. This is consistent with higher vibrational scattering at the larger pores in the *y*-direction, which comparatively reduces the effect of phonon-phonon scattering in that direction. Note, the ABTPA chains are oriented at an angle of  $\sim 26^\circ$  with the *x*-*y* plane (see Fig. S1c). The hydrogen bonds are stacked along the *z*-direction with the polymer chains at an angle of  $\sim 64^\circ$  with the *z*-direction. Therefore, throughout the temperature range as shown in Fig. 3, the thermal conductivity is the lowest along the *z*-direction. Taken together, these results suggest the possibility of tuning the thermal conductivity in these HOFs through proper design of the pore geometry, polymer chain orientation and placement of the hydrogen bonds in the organic framework. In what follows, we will show that the dynamic response of the hydrogen bonds along with the flexibility of the molecular building blocks under application of external strain can be used to align (or misalign) the building blocks along a particular direction to increase (or decrease) the thermal conductivity in these materials.

We note that in our previous study on the thermal properties of 2D COFs,<sup>11</sup> we have shown that the layered structure of COFs with strong covalent bonds in the in-plane direction and weaker supramolecular interactions in the through-plane direction results in a higher thermal conductivity anisotropy ratio in 2D COFs as compared to HOFs. However, what separates HOFs in comparison to the 2D COFs is the fact that the thermal conductivity can vary in all three principle directions, whereas the thermal conductivity along the bonded plane remains similar for 2D COFs. Moreover, 3D COFs and MOFs (such as COF-300 and MOF-5) demonstrate isotropic thermal conductivities

of  $\sim 0.3 \text{ W m}^{-1} \text{ K}^{-1}$  in all three principle directions.<sup>46,47</sup> Therefore, this unique physical attribute where the thermal conductivity can change by a factor of 3 depending on the crystalline direction separates HOFs from other organic framework-based materials, where achieving anisotropy in all three principle directions has not been realized so far.

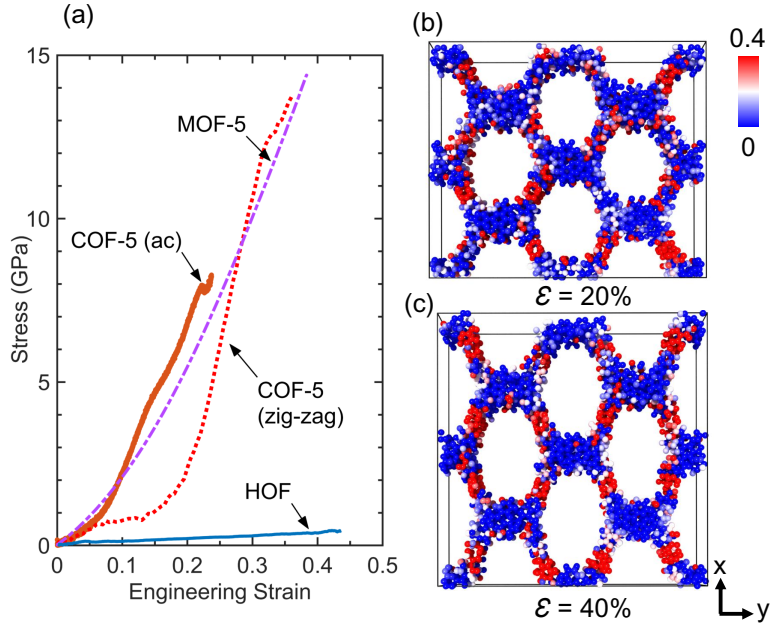


Figure 4: (a) Comparison of the stress-strain relationships for COF-5 (taken from Ref. 11) under uniaxial tension in the zig-zag and arm-chair directions, MOF-5 (from additional simulations performed with the model as described in Ref. 31), and our ABTPA HOF under uniaxial tension in the  $x$ -direction. Snapshots of the computational domains at uniaxial strain levels of (b) 20% and (c) 40%. The atoms are colored based on their atomic level strain relative to the relaxed structure. Stress localization (represented by the red colored atoms) is mainly concentrated around the hydrogen-bonding interactions for the strain levels, which shows the dynamic and responsive nature of these non-bonded interactions to absorb the stress in the framework.

The ultraflexible nature of these framework materials are revealed by monitoring their stress response to tensile loading. This is shown in Fig. 4a, where we plot the stress-strain response of the HOF under uniaxial tension in the  $x$ -direction; stress-strain curves for the other directions are given in the Supporting Information. We observe that the stress build-up in the structure is minimal due to the applied tensile loading even for strain levels of  $\sim 40\%$ , after which a catastrophic breakdown of the structure occurs that originates at the dynamic hydrogen-bonded interactions (Fig. S8). This unique ultraflexible mechanical response of ABTPA HOF to tensile loading can be better appre-

ciated by comparison to the strain response of other organic framework materials (i.e. MOFs and COFs) as shown in Fig. 4a. Note, we calculate the stress-strain response for MOF-5 based on the model described in Ref. 31. For MOF-5, we observe a monotonically increasing stress response due to the application of strain. Similarly, we also include the stress-strain curves for COF-5 as calculated in our previous work.<sup>11</sup> Although COF-5 displays an overall better flexibility as compared to the MOF-5 structure, for both types of frameworks there is a considerable buildup of stress due to the application of a uniaxial strain, which is in contrast to the response of our HOF structure.

We can attribute this ultraflexible response of HOFs to the ability of the hydrogen bonds to locally absorb the stress when strained in a particular direction. This is highlighted in Fig. 4b and 4c, where the atoms are colored based on their von Mises strain under uniaxial tensile strains of 20% and 40% along the  $x$ -direction, respectively. As uniaxial strain is increased, stress localization mainly occurs near the O-H $\cdots$ O hydrogen bonds (as represented by the red colored atoms). Through the dynamic response of the large number of these non-covalent interactions forming the hydrogen-bonded network, these structures are endowed with the unique ability to locally absorb the applied stress. In our previous work in Ref. 11, a similar mechanism was shown for COF-5, where the stress localization occurred around the linkers of the COF-5, ultimately leading to catastrophic failure. For our HOFs, however, the build-up of stress around the dynamic hydrogen-bonded interactions not only leads to the ultraflexible nature of these organic frameworks, but also endows them with the ability to absorb high levels of strain without compromising their structural integrity.

Next, to investigate the effect of strain on the thermal response of the ABTPA HOF, we plot the thermal conductivity in the three principle directions at different strain levels when tensile loading is applied along the  $x$ - and  $z$ -directions as shown in Fig. 5a and Fig. 5b, respectively. When strained in the  $x$ -direction, the thermal conductivity is reduced slightly in the  $z$ -direction, while, the thermal conductivities in the  $x$ - and  $y$ -directions are largely unaffected for the entire range of tensile strain. The reduction in the  $z$ -direction can be expected since the computational domain contracts significantly in that direction causing the organic building blocks to preferentially align perpendicular to

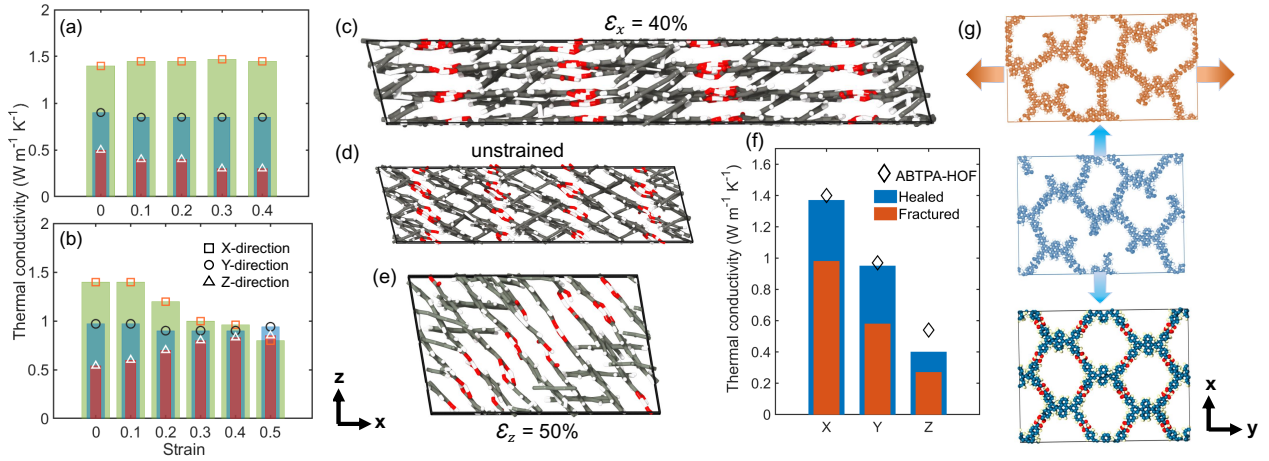


Figure 5: Change in the thermal conductivity in the three principal directions as a function of applied uniaxial strain along the (a)  $x$ -direction and (b)  $z$ -direction. Snapshots of the cross-section of the  $x$ - $z$  plane showing the arrangement of polymer chains under (c) uniaxial strain along the  $x$ -direction at 40% strain level, (d) unstrained conditions, and (e) when uniaxial strain is applied along the  $z$ -direction at 50% strain level. The organic building blocks align parallel to the direction of the applied strain, which facilitates heat transfer. However, when strain is applied in the  $x$ -direction, the counter effect of increase in the pore size results in negligible change in the thermal conductivity along that direction. (f) Thermal conductivity along the three principal directions for the cases when our HOF breaks down under uniaxial tension and when the structure regains its' framework integrity through an application of a counter strain in the opposite lateral direction. (g) Snapshots of our computational domain showing the sequence of catastrophic breakdown of the framework as uniaxial tension is applied along the  $y$ -direction and the 'self-healing' process when a counter strain is applied along the  $x$ -direction.

the  $z$ -axis (see Fig. 5c). Although the application of tensile strain along the  $x$ -direction leads to an overall better alignment of the organic building blocks along the  $x$ - $y$  plane, it also causes the overall pore size to increase considerably (see Fig. S7b and Fig. S7c), thus countering the effect of chain alignment on the thermal conductivity. This is in-line with our prior works that have shown that the increase in pore size results in a reduced thermal conductivity in organic framework materials due to vibrational scattering at the pore walls.<sup>11,48</sup> Similarly, when tensile loading is applied along the  $z$ -direction, the organic building blocks now orient better along that direction (see Figs. 5d and 5e) leading to an enhanced thermal conductivity, which monotonically increases as strain is increased by up to  $\sim 30\%$ . In the  $x$ -direction, however, there is a considerable amount of misalignment of the polymer chains (more-so than in the  $y$ -direction) as the computational domain contracts substantially more in that direction (see Fig. S5b), which leads to the reduction in thermal conductivity as tensile strain is increased in that direction. Taken together, our uniaxial tensile simulations show the ultraflexible nature of these framework materials, where the dynamic movement of the organic building blocks, facilitated by the responsive hydrogen-bonding interactions, can be used to tailor their anisotropic thermal properties.

Finally, we demonstrate the ‘self-healing’ nature of these frameworks to recover from catastrophic breakdown of their framework structure. This is realized through a counter strain that we apply in the lateral direction after the framework fractures. Note, the counter strain is applied in the direction where the computational domain contracts during uniaxial tension. Although in our simulations, we can visually identify when the structure regains its’ original framework due to the counter strain, an important aspect of ‘self-healing’ is the restoration of initial physical properties through dynamic response to an external stimulus.<sup>49</sup> This is quantified by calculating the thermal conductivity of our ‘healed’ HOF structure as shown in Fig. 5f. The thermal conductivity is considerably lower in all three principle directions when the hydrogen bonds are broken due to tensile strain; as shown in the top panel of Fig. 5g, the HOF structure fractures at  $\sim 15\%$  strain when tensile force is applied along the  $y$ -direction. When a counter strain is applied in the  $x$ -direction, the hydrogen bonds ‘heal’ and the structure regains its’ original shape. Along with the framework

structure, the application of the counter strain is able to regain the intrinsic thermal conductivities in all three principle directions as shown in Fig. 5f, which demonstrates the ‘self-healing’ nature of these HOFs that are coupled to fast and efficient cross-linking reactions. We note this ‘self-healing’ attribute is also observed when the initial tensile strain is applied in the *x*-direction and the counter strain is applied in the *y*-direction (see Fig. S10). This ‘self-healing’ nature separates HOFs from other organic-based framework materials such as COFs and MOFs, where this dynamic and reversible change in physical properties has not been demonstrated as of yet.

The design of polymeric materials with the capability to efficiently and actively manipulate heat conduction on-demand has been of interest for a range of applications such as in shape-programmable structures, artificial skin, flexible electronics, and soft robotics.<sup>50–52</sup> The demonstration of HOFs with the unique ability to ‘self-heal’ in this work could potentially lead to their application in the aforementioned technologies to dynamically switch between the high thermal conductivity state (with an extended periodic framework structure) and low thermal conductivity state (when the hydrogen-bonded interactions are broken). For polymeric materials, dynamic control of vibrational thermal conductivity has been limited to light-triggered phase transitions in azopolymers, which show a very slow response time ( $\sim 10$  s) to switch between a low thermal conductivity state of  $0.1 \text{ W m}^{-1} \text{ K}^{-1}$  to a high thermal conductivity state of  $0.35 \text{ W m}^{-1} \text{ K}^{-1}$ .<sup>53</sup> While the thermal conductivities for HOFs are relatively higher as compared to the azopolymers, for thermal management applications, it is desirable for soft polymeric materials to demonstrate metal-like thermal conductivities.<sup>51</sup> In this regard, new strategies such as interpenetration or guest-host interactions could potentially enhance the heat transfer efficacy in these types of polymeric framework materials, which could potentially lead to unprecedented, dynamic thermal responses.<sup>47,48,54</sup>

In summary, our systematic atomistic simulations based on reactive MD simulations show that HOFs are capable of possessing high thermal conductivities for porous materials, which mainly depend on the orientation of their ultraflexible organic building blocks. Specifically, when uniaxial tension is applied along a direction, the building blocks preferentially align along that direction to facilitate heat transfer. We attribute their ultraflexible framework to the abundance and reversible

nature of hydrogen-bonded interactions that makeup the framework and are capable of absorbing and localizing the stress under highly strained conditions. We also reveal their unique ‘self-healing’ characteristics where the framework is able to recover the thermal conductivity even when the structure experiences catastrophic fracture. Our results shed light on the anisotropic nature of the thermo-mechanical properties of ABTPA HOF and show that their responsive nature to external stimuli can be harnessed for applications such as thermal switches.

## Acknowledgement

This work is supported by the Office of Naval Research, Grant No. N00014-21-1-2622. The work is also partially supported by the National Science Foundation (NSF Award No. 2119365).

## Supporting Information Available

The Supporting information is available free of charge at .

- Details of the computational domain setup, equilibrium molecular dynamics approach, vibrational density of states calculations, and tensile strain simulations.

## References

- (1) Xie, Z.; Hu, B.-L.; Li, R.-W.; Zhang, Q. Hydrogen bonding in self-healing elastomers. *ACS omega* **2021**, *6*, 9319–9333.
- (2) Rich, S. I.; Wood, R. J.; Majidi, C. Untethered soft robotics. *Nature Electronics* **2018**, *1*, 102–112.
- (3) Evans, A. M.; Giri, A.; Sangwan, V. K.; Xun, S.; Bartnof, M.; Torres-Castanedo, C. G.; Balch, H. B.; Rahn, M. S.; Bradshaw, N. P.; Vitaku, E., et al. Thermally conductive ultra-low-

k dielectric layers based on two-dimensional covalent organic frameworks. *Nature materials* **2021**, *20*, 1142–1148.

- (4) Reb, L. K.; Böhmer, M.; Predeschly, B.; Grott, S.; Weindl, C. L.; Ivandekic, G. I.; Guo, R.; Dreißigacker, C.; Gernhäuser, R.; Meyer, A., et al. Perovskite and organic solar cells on a rocket flight. *Joule* **2020**, *4*, 1880–1892.
- (5) Giri, A.; Hopkins, P. E. Achieving a better heat conductor. *Nature Materials* **2020**, *19*, 482–484.
- (6) Liu, H.; Wang, L.; Lin, G.; Feng, Y. Recent progress in the fabrication of flexible materials for wearable sensors. *Biomater. Sci.* **2022**, *10*, 614–632.
- (7) Wu, J.; Xu, F.; Li, S.; Ma, P.; Zhang, X.; Liu, Q.; Fu, R.; Wu, D. Porous polymers as multifunctional material platforms toward task-specific applications. *Advanced Materials* **2019**, *31*, 1802922.
- (8) Li, B.; Wen, H.-M.; Cui, Y.; Zhou, W.; Qian, G.; Chen, B. Emerging multifunctional metal–organic framework materials. *Advanced Materials* **2016**, *28*, 8819–8860.
- (9) Huang, N.; Wang, P.; Jiang, D. Covalent organic frameworks: a materials platform for structural and functional designs. *Nature Reviews Materials* **2016**, *1*, 1–19.
- (10) Li, P.; Ryder, M. R.; Stoddart, J. F. Hydrogen-bonded organic frameworks: a rising class of porous molecular materials. *Accounts of Materials Research* **2020**, *1*, 77–87.
- (11) Giri, A.; Evans, A. M.; Rahman, M. A.; McGaughey, A. J.; Hopkins, P. E. Highly Negative Poisson’s Ratio in Thermally Conductive Covalent Organic Frameworks. *ACS nano* **2022**, *16*, 2843–2851.
- (12) Zhang, H.; Zhang, C.; Ji, W.; Wang, X.; Li, Y.; Tao, W. Experimental characterization of the thermal conductivity and microstructure of opacifier-fiber-aerogel composite. *Molecules* **2018**, *23*, 2198.

(13) Huang, B.; McGaughey, A.; Kaviany, M. Thermal conductivity of metal-organic framework 5 (MOF-5): Part I. Molecular dynamics simulations. *International journal of heat and mass transfer* **2007**, *50*, 393–404.

(14) Zhang, X.; Jiang, J. Thermal conductivity of zeolitic imidazolate framework-8: A molecular simulation study. *The Journal of Physical Chemistry C* **2013**, *117*, 18441–18447.

(15) Laurenz, E.; Füldner, G.; Velte, A.; Schnabel, L.; Schmitz, G. Frequency response analysis for the determination of thermal conductivity and water transport in MOF adsorbent coatings for heat transformation. *International Journal of Heat and Mass Transfer* **2021**, *169*, 120921.

(16) Babaei, H.; DeCoster, M. E.; Jeong, M.; Hassan, Z. M.; Islamoglu, T.; Baumgart, H.; McGaughey, A. J.; Redel, E.; Farha, O. K.; Hopkins, P. E., et al. Observation of reduced thermal conductivity in a metal-organic framework due to the presence of adsorbates. *Nature communications* **2020**, *11*, 1–8.

(17) Wang, X.; Guo, R.; Xu, D.; Chung, J.; Kaviany, M.; Huang, B. Anisotropic lattice thermal conductivity and suppressed acoustic phonons in MOF-74 from first principles. *The Journal of Physical Chemistry C* **2015**, *119*, 26000–26008.

(18) Coquil, T.; Lew, C. M.; Yan, Y.; Pilon, L. Thermal conductivity of pure silica MEL and MFI zeolite thin films. *Journal of Applied Physics* **2010**, *108*, 044902.

(19) McGaughey, A.; Kaviany, M. Thermal conductivity decomposition and analysis using molecular dynamics simulations: Part II. Complex silica structures. *International Journal of Heat and Mass Transfer* **2004**, *47*, 1799–1816.

(20) Hanif, S.; Sultan, M.; Miyazaki, T. Effect of relative humidity on thermal conductivity of zeolite-based adsorbents: Theory and experiments. *Applied Thermal Engineering* **2019**, *150*, 11–18.

(21) Murashov, V. V. Thermal conductivity of model zeolites: molecular dynamics simulation study. *Journal of Physics: Condensed Matter* **1999**, *11*, 1261.

(22) Davis, M. E. Ordered porous materials for emerging applications. *Nature* **2002**, *417*, 813–821.

(23) Slater, A. G.; Cooper, A. I. Function-led design of new porous materials. *Science* **2015**, *348*, aaa8075.

(24) Little, M. A.; Cooper, A. I. The chemistry of porous organic molecular materials. *Advanced Functional Materials* **2020**, *30*, 1909842.

(25) Lehn, J.-M. Towards complex matter: supramolecular chemistry and self-organization. *European Review* **2009**, *17*, 263–280.

(26) Wang, B.; Lin, R.-B.; Zhang, Z.; Xiang, S.; Chen, B. Hydrogen-bonded organic frameworks as a tunable platform for functional materials. *Journal of the American Chemical Society* **2020**, *142*, 14399–14416.

(27) Lin, R.-B.; He, Y.; Li, P.; Wang, H.; Zhou, W.; Chen, B. Multifunctional porous hydrogen-bonded organic framework materials. *Chemical Society Reviews* **2019**, *48*, 1362–1389.

(28) Wilson, A. J. Non-covalent polymer assembly using arrays of hydrogen-bonds. *Soft Matter* **2007**, *3*, 409–425.

(29) Yan, X.; Wang, F.; Zheng, B.; Huang, F. Stimuli-responsive supramolecular polymeric materials. *Chemical Society Reviews* **2012**, *41*, 6042–6065.

(30) Babaei, H.; McGaughey, A. J.; Wilmer, C. E. Effect of pore size and shape on the thermal conductivity of metal-organic frameworks. *Chemical science* **2017**, *8*, 583–589.

(31) Babaei, H.; Wilmer, C. E. Mechanisms of Heat Transfer in Porous Crystals Containing Adsorbed Gases: Applications to Metal-Organic Frameworks. *Phys. Rev. Lett.* **2016**, *116*, 025902.

(32) Han, L.; Budge, M.; Greaney, P. A. Relationship between thermal conductivity and framework architecture in MOF-5. *Computational materials science* **2014**, *94*, 292–297.

(33) Huang, B.; Ni, Z.; Millward, A.; McGaughey, A.; Uher, C.; Kaviany, M.; Yaghi, O. Thermal conductivity of a metal-organic framework (MOF-5): Part II. Measurement. *International Journal of Heat and Mass Transfer* **2007**, *50*, 405–411.

(34) Wieme, J.; Vandenbrande, S.; Lamine, A.; Kapil, V.; Vanduyfhuys, L.; Van Speybroeck, V. Thermal engineering of metal-organic frameworks for adsorption applications: a molecular simulation perspective. *ACS applied materials & interfaces* **2019**, *11*, 38697–38707.

(35) Babaei, H.; McGaughey, A. J.; Wilmer, C. E. Transient mass and thermal transport during methane adsorption into the metal-organic framework HKUST-1. *ACS applied materials & interfaces* **2018**, *10*, 2400–2406.

(36) DeCoster, M. E.; Babaei, H.; Jung, S. S.; Hassan, Z. M.; Gaskins, J. T.; Giri, A.; Tiernan, E. M.; Tomko, J. A.; Baumgart, H.; Norris, P. M.; McGaughey, A. J. H.; Wilmer, C. E.; Redel, E.; Giri, G.; Hopkins, P. E. Hybridization from Guest–Host Interactions Reduces the Thermal Conductivity of Metal–Organic Frameworks. *Journal of the American Chemical Society* **2022**, *144*, 3603–3613.

(37) Erickson, K. J.; Léonard, F.; Stavila, V.; Foster, M. E.; Spataru, C. D.; Jones, R. E.; Foley, B. M.; Hopkins, P. E.; Allendorf, M. D.; Talin, A. A. Thin film thermoelectric metal–organic framework with high Seebeck coefficient and low thermal conductivity. *Advanced Materials* **2015**, *27*, 3453–3459.

(38) Lamine, A.; Wieme, J.; Hoffman, A. E.; Van Speybroeck, V. Atomistic insight in the flexibility and heat transport properties of the stimuli-responsive metal–organic framework MIL-53 (Al) for water-adsorption applications using molecular simulations. *Faraday Discussions* **2021**, *225*, 301–323.

(39) Zhang, S.; Liu, J.; Liu, L. Insights into the thermal conductivity of MOF-5 from first principles. *RSC advances* **2021**, *11*, 36928–36933.

(40) Cheng, R.; Li, W.; Wei, W.; Huang, J.; Li, S. Molecular Insights into the Correlation between Microstructure and Thermal Conductivity of Zeolitic Imidazolate Frameworks. *ACS Applied Materials & Interfaces* **2021**, *13*, 14141–14149.

(41) Ying, P.; Zhang, J.; Zhong, Z. Effect of Phase Transition on the Thermal Transport in Isoreticular DUT Materials. *The Journal of Physical Chemistry C* **2021**, *125*, 12991–13001.

(42) Huang, J.; Xia, X.; Hu, X.; Li, S.; Liu, K. A general method for measuring the thermal conductivity of MOF crystals. *International Journal of Heat and Mass Transfer* **2019**, *138*, 11–16.

(43) Cui, P.; Svensson Grape, E.; Spackman, P. R.; Wu, Y.; Clowes, R.; Day, G. M.; Inge, A. K.; Little, M. A.; Cooper, A. I. An expandable hydrogen-bonded organic framework characterized by three-dimensional electron diffraction. *Journal of the American Chemical Society* **2020**, *142*, 12743–12750.

(44) Chenoweth, K.; van Duin, A. C. T.; Goddard, W. A. ReaxFF Reactive Force Field for Molecular Dynamics Simulations of Hydrocarbon Oxidation. *The Journal of Physical Chemistry A* **2008**, *112*, 1040–1053.

(45) Plimpton, S. Fast parallel algorithms for short-range molecular dynamics. *Journal of Computational Physics* **1995**, *117*, 1–19.

(46) Huang, B. L.; McGaughey, A. J. H.; Kaviany, M. Thermal conductivity of metal-organic framework 5 (MOF-5): Part I. Molecular dynamics simulations. *International Journal of Heat and Mass Transfer* **2007**, *50*, 393–404.

(47) Dionne, C. J.; Rahman, M. A.; Hopkins, P. E.; Giri, A. Supramolecular Interactions Lead to

Remarkably High Thermal Conductivities in Interpenetrated Two-Dimensional Porous Crystals. *Nano Letters* **2022**, *22*, 3071–3076.

(48) Rahman, M. A.; Dionne, C. J.; Giri, A. Pore Size Dictates Anisotropic Thermal Conductivity of Two-Dimensional Covalent Organic Frameworks with Adsorbed Gases. *ACS Applied Materials & Interfaces* **2022**, *14*, 21687–21695.

(49) Binder, W. H. *Self-Healing Polymers*; Wiley, New York, 2013.

(50) Xu, Y.; Wang, X.; Zhou, J.; Song, B.; Jiang, Z.; Lee, E. M. Y.; Huberman, S.; Gleason, K. K.; Chen, G. Molecular engineered conjugated polymer with high thermal conductivity. *Science Advances* **2018**, *4*, eaar3031.

(51) Xu, Y.; Kraemer, D.; Song, B.; Jiang, Z.; Zhou, J.; Loomis, J.; Wang, J.; Li, M.; Ghasemi, H.; Huang, X.; Li, X.; Chen, G. Nanostructured polymer films with metal-like thermal conductivity. *Nature Communications* **2019**, *10*, 1771.

(52) Bartlett, M. D.; Kazem, N.; Powell-Palm, M. J.; Huang, X.; Sun, W.; Malen, J. A.; Majidi, C. High thermal conductivity in soft elastomers with elongated liquid metal inclusions. *Proceedings of the National Academy of Sciences* **2017**, *114*, 2143–2148.

(53) Shin, J.; Sung, J.; Kang, M.; Xie, X.; Lee, B.; Lee, K. M.; White, T. J.; Leal, C.; Sottos, N. R.; Braun, P. V.; Cahill, D. G. Light-triggered thermal conductivity switching in azobenzene polymers. *Proceedings of the National Academy of Sciences* **2019**, *116*, 5973–5978.

(54) Sezginel, K. B.; Asinger, P. A.; Babaei, H.; Wilmer, C. E. Thermal Transport in Interpenetrated Metal–Organic Frameworks. *Chemistry of Materials* **2018**, *30*, 2281–2286.

## Graphical TOC Entry

